Supporting Information

Hinohara et al. 10.1073/pnas.1113271109

SI Results

Effects of Tyrosine Kinase Inhibitors on NF-κB Activity and Mammosphere Formation. We assessed the effects of tyrosine kinase inhibitors on the NF-κB activity and mammosphere-forming ability of MCF7 cells. The following tyrosine kinase inhibitors were used: lapatinib, which inhibits EGF receptor (EGFR) and ErbB2; gefitinib, which inhibits EGFR; dasatinib, which inhibits Src; and sunitinib. We treated MCF7 cells with HRG together with these inhibitors. Treatment with lapatinib decreased NF-κB activity and mammosphere formation, whereas the other tyrosine kinase inhibitors did not significantly affect NF-κB activity and mammosphere formation (Fig. S2 *A* and *B*). DHMEQ plus lapatinib had an additive effect on the inhibition of mammosphere formation (Fig. S2*C*).

NF-κB Regulates Mammosphere Formation in EGF/bFGF/B27-Containing Medium. Treatment with EGF/bFGF/B27 did not significantly induce phosphorylation of ErbB2/ErbB3, but it did induce strong phosphorylation of the FGF receptor substrate 2α (FRS2α), a membrane-anchored docking protein involved in FGF signaling (Fig. S4*A*) (1, 2). Furthermore, bFGF but not EGF increased mammosphere formation (Fig. S4*B*), suggesting that MCF7 mammosphere growth in the presence of EGF/bFGF/B27 is dependent on bFGF rather than EGF. Consistent with this result, the expression level of EGFR was low in MCF7 cells (Fig. S4*A*). Compared with adherent cells, we found that the NF-κB activities were higher in mammosphere cells cultured with EGF/bFGF/B27 (Fig. S5*A*). We then cultured mammospheres in the presence of DHMEQ with EGF/bFGF/B27. Treatment with DHMEQ decreased the number of both primary and secondary mammospheres (Fig. S5*B*). In addition, the expression of the IκBα mutant resulted in a decreased frequency of mammosphere formation during serial passages (Fig. S5*C*). These results further support the role of NF-κB in regulating mammosphere formation.

SI Materials and Methods

Mammosphere Assay Performed with Different Cell-Plating Densities. We performed mammosphere assays with primary tumor cells from breast cancer patients. Cells were plated at the density of 5,000 cells/mL in six-well plates or 50 cells/100 μL per well in 96-well plates (500 cells/mL). If the mammospheres were derived from clonal expansion of single cells rather than aggregation, the frequencies of mammosphere formation were expected to be fairly constant irrespective of cell-plating density. Under conditions of 50 cells per well, we observed only single mammospheres in 19.0 ± 1.0 wells and 17.3 ± 1.5 wells per 96-well plate when cultured with EGF/bFGF/B27 or HRG, respectively. Because each well contained only one mammosphere, this result yielded mammosphere-forming frequencies of 0.40% ± 0.02% and 0.36% ± 0.03% when cultured with EGF/bFGF/B27 or HRG, respectively. When tumor cells from the same patient were plated at 5,000 cells/mL, the mammosphere-forming frequencies were 0.37% ± 0.04% in the presence of EGF/bFGF/B27 and 0.30% ± 0.02% in the presence of HRG. These data suggest that the mammospheres cultured at densities of 5,000 cells/mL or less are clonally derived from single cells. This result is consistent with the previous report (3).

Xenografts. Eight-week-old female NOD/SICD mice were anesthetized with isoflurane (Abbott Japan), and 60 d-release β-estradiol (E2) pellets containing 0.72 mg of E2 (Innovative Research of America) were s.c. implanted on the back of the neck. A total of 1×10^5 MCF7 cells expressing the indicated constructs were suspended in 1:1 volumes of PBS (PBS)/Matrigel (BD Biosciences) to produce 100 μL of the cell mixture that was subsequently injected into the mammary fat pads.

Construction of Lentiviral Vectors. Plasmids containing cDNA encoding mutant IκBα (IκBαSR) were cloned into a CSII-EF-MCS-IRES2-Venus vector that was a kind gift from H. Miyoshi (RIKEN, Tsukuba, Japan) by standard molecular biological techniques (4). The CSII-EF-MCS-IRES2-Venus vector is a plasmid with a gene encoding d2Venus (5) (provided by A. Miyawaki, RIKEN, Wako, Japan). Viral supernatant was produced by cotransfecting CSII-EF-MCS-IRES2-Venus vector with packaging plasmid pCMV-VSV-G-RSV-Rev and pCAG-HIVgp in 293T cells by using lipofectamine (Invitrogen), as previously described (6). The viral titers were determined by transducing HeLa cells at serial dilutions and analyzed by the amount of integrated DNA measured by the quantitative real-time PCR method (DNA titer). High-titer viral stocks were prepared by ultracentrifugation.

Transduction of Cells with Lentiviral Vectors. Cells were pelleted and infected with viral supernatant containing 5 μg/mL polybrene (Millipore) at a multiplicity of infection of 1:10 and then incubated for 3 h at 37 °C in 5% CO_2.

Immunoblot Analysis and Immunoprecipitation. Western blotting was performed by standard procedures. All antibodies were purchased from Cell Signaling Technology and used at a 1:1,000 dilution, unless otherwise noted. Antibodies against the following proteins were used: ErbB2, p-ErbB2, ErbB3, p-ErbB3, Akt, p-Akt, Erk1/2, p-Erk1/2, IKKα, IKKβ, p-IKKα/β, IκBα, p-IκBα, RELA (1:2,000 dilution), p-RELA, FRS2α (1:100 dilution; Santa Cruz), p-FRS2α, and actin (1:5,000 dilution; Millipore). For immunoprecipitation, cell lysates were precleared with protein G–Sepharose beads (GE Healthcare) for 1h and then incubated for 1 h on ice with rabbit monoclonal antibody to ErbB2, after which protein G–Sepharose beads were added and the mixture was incubated for an additional 1 h. The beads were isolated by centrifugation and washed three times with lysis buffer, after which the bead-bound proteins were subjected to immunoblot analysis.

Quantification of NF-κB Activity. Nuclear extracts were prepared with a Nuclear Extract kit (Active Motif), and NF-κB RELA-DNA binding activity was measured with a TransAM NF-κB p65 Transcription Factor Assay kit (Active Motif) according to the manufacturer's protocol.

Quantitative Real-Time PCR. Total RNA was prepared by using TRIzol Reagent (Invitrogen) and then transcribed into cDNA with a High Capacity cDNA Reverse Transcription kit (Applied Biosystems). Quantitative RT-PCR was performed with Taqman probes from Applied Biosystems, according to the manufacturer's recommendations. Reactions were performed in an Applied Biosystems StepOne real-time PCR system.

Cell-Cycle Analysis. Mammosphere cells were fixed in 70% ethanol for 2 h at 4 °C. They were washed twice with PBS, followed by RNase treatment (0.25 mg/mL) and PI (50 μg/mL) staining for 15 min at 37 °C in the dark. Cell-cycle analysis was performed by using a FACSAria Cell Sorter (BD Bioscience).

1. Eswarakumar VP, Lax I, Schlessinger J (2005) Cellular signaling by fibroblast growth factor receptors. *Cytokine Growth Factor Rev* 16:139–149.
2. Gotoh N (2008) Regulation of growth factor signaling by FRS2 family docking/scaffold adaptor proteins. *Cancer Sci* 99:1319–1325.
3. Pece S, et al. (2010) Biological and molecular heterogeneity of breast cancers correlates with their cancer stem cell content. *Cell* 140:62–73.
4. Miyoshi H, Smith KA, Mosier DE, Verma IM, Torbett BE (1999) Transduction of human CD34+ cells that mediate long-term engraftment of NOD/SCID mice by HIV vectors. *Science* 283:682–686.
5. Nagai T, et al. (2002) A variant of yellow fluorescent protein with fast and efficient maturation for cell-biological applications. *Nat Biotechnol* 20:87–90.
6. Murohashi M, et al. (2010) Gene set enrichment analysis provides insight into novel signalling pathways in breast cancer stem cells. *Br J Cancer* 102:206–212.

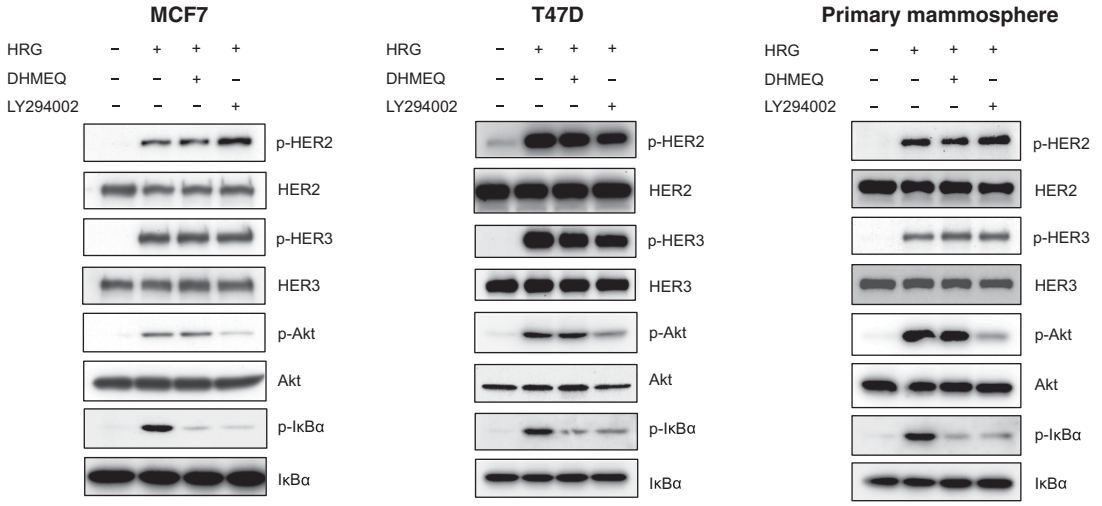

Fig. S1. Effect of DHMEQ and LY294002 on phosphorylation of Akt and IκBα. MCF7, T47D, and primary mammosphere cells were treated with 5 μg/mL DHMEQ (NF-κB inhibitor) or 5 μM LY294002 (PI3K inhibitor) for 1 h, and then the cells were treated with 100 ng/mL HRG for 30 min. The levels of p-ErbB2, ErbB2, p-ErbB3, ErbB3, p-Akt, Akt, p-IκBα, and IκBα were determined by immunoblotting. DHMEQ decreased the phosphorylation of IκBα, whereas LY294002 inhibited the phosphorylation of both Akt and IκBα.

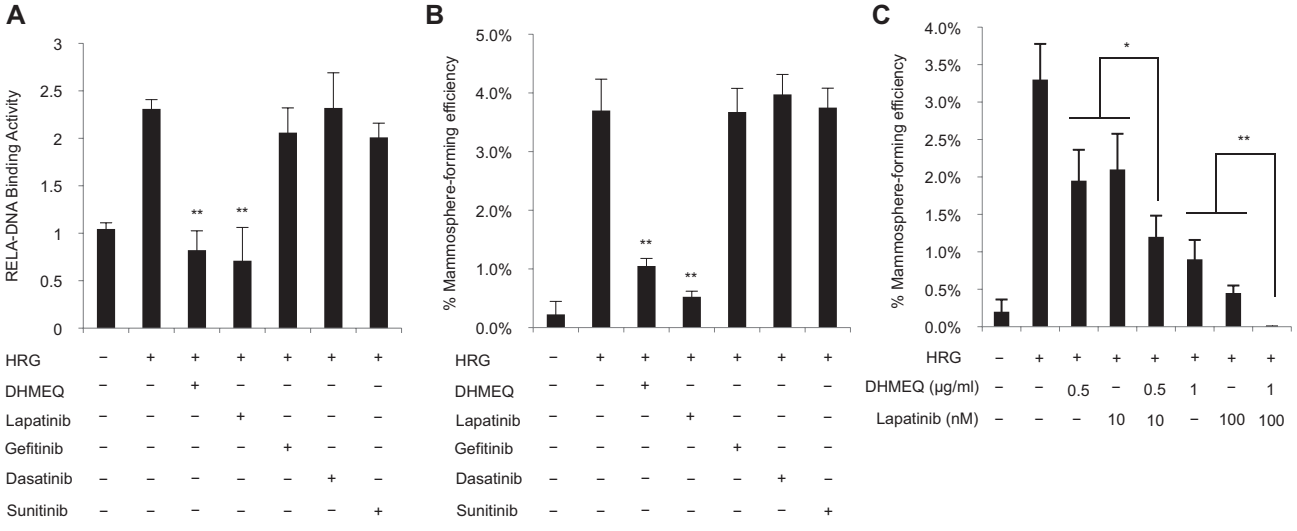

Fig. S2. Effect of tyrosine kinase inhibitors on mammosphere formation and NF-κB activity. (*A*) MCF7 cells were treated with 1 μg/mL DHMEQ, 100 nM lapatinib, 100 nM gefitinib, 100 nM dasatinib, and 100 nM sunitinib for 1 h, and then the cells were treated with 100 ng/mL HRG for 1 h. The DNA-binding activity of RELA was quantified by ELISA [data are mean ± SD; $n = 3$, $^{**}P < 0.01$, relative to the values in the HRG(+)]. (*B*) MCF7 cells were incubated with 20 ng/mL HRG with or without 1 μg/mL DHMEQ, 100 nM lapatinib, 100 nM gefitinib, 100 nM dasatinib or 100 nM sunitinib. The number of formed mammospheres was counted, and the percentage of mammosphere-forming cells was determined [data are mean ± SD; $n = 3$, $^{**}P < 0.01$, relative to the values in the HRG(+)]. (*C*) To examine the combinatory effect of DHMEQ and lapatinib, MCF7 cells were incubated with 20 ng/mL HRG with or without the indicated concentration of DHMEQ and lapatinib (data are mean ± SD; $n = 3$, $^{*}P < 0.05$, $^{**}P < 0.01$).

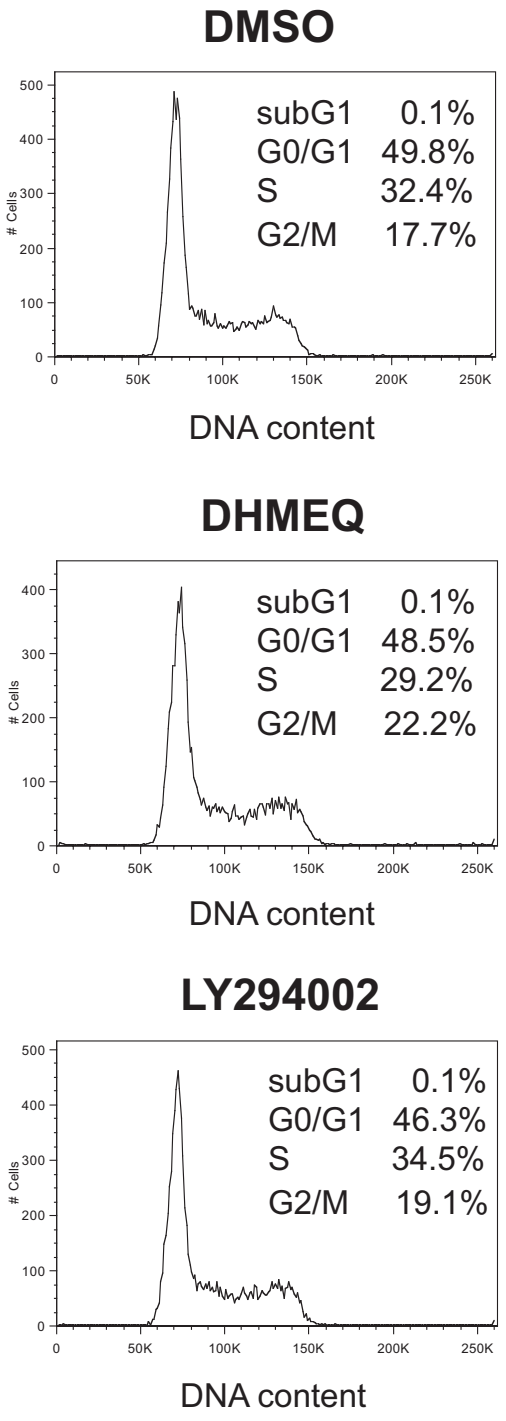

Fig. S3. Determination of apoptosis by DHMEQ in MCF7 mammosphere cells. To elucidate the apoptotic effect of DHMEQ, HRG-induced MCF7 mammosphere cells were incubated with DMSO, 1 μg/mL of DHMEQ, or 1 μM LY294002 for 4 d. Ethanol-fixed cells were then stained with propidium iodide (PI) and subjected to DNA content analysis by flow cytometry. The percentages of cells in the sub G1, G0/G1, S, and G2/M phase are indicated. DHMEQ and LY294002 had no effect on apoptosis (sub G1) at the effective concentrations for mammosphere formation.

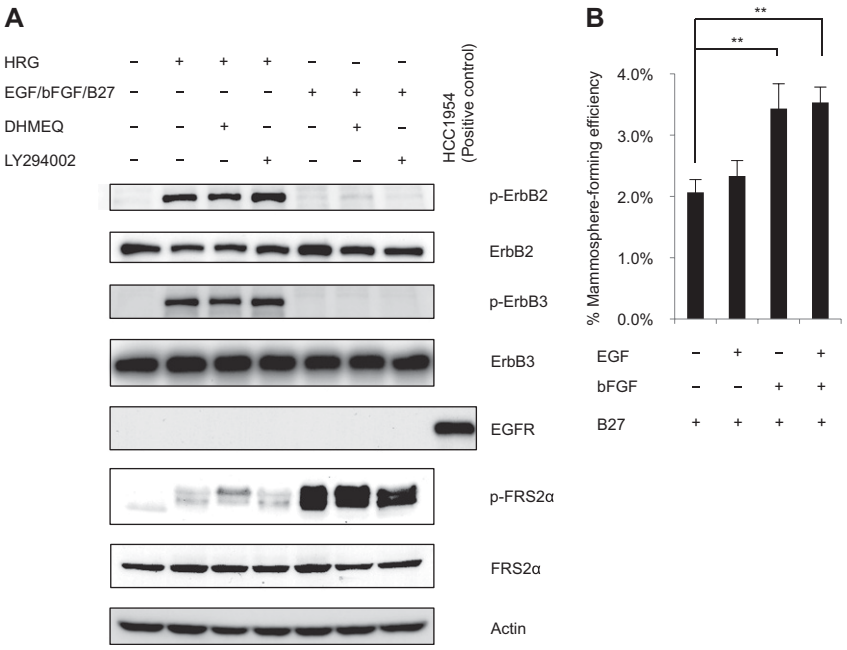

Fig. S4. The role of FGF signaling on mammosphere formation. (*A*) MCF7 mammosphere cells were treated with 5 μg/mL DHMEQ or 5 μM LY294002 for 1 h, and then the cells were treated with 20 ng/mL HRG or EGF/bFGF/B27 for 30 min. Protein expression levels were determined by immunoblotting. HRG induced the phosphorylation of ErbB2 and ErbB3, whereas EGF/bFGF/B27 did not. Treatment with EGF/bFGF/B27 induced the phosphorylation of FRS2α, a membrane-anchored docking protein involved in the activation of FGF receptor signaling. (*B*) MCF7 cells were incubated with B27 in combination with EGF, bFGF, or both, and the formed mammospheres were counted. Treatment with bFGF increased mammosphere formation (data are mean ± SD; $n = 3$, $^{**}P < 0.01$).

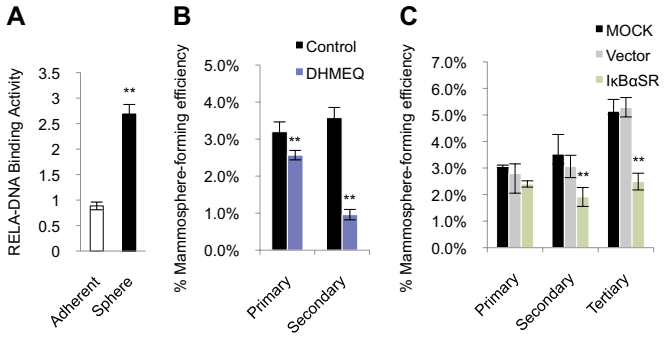

Fig. S5. The role of NF-κB on mammosphere formation in EGF/bFGF/B27-containing medium. (*A*) The DNA-binding activity of RELA was quantified by ELISA (data are mean ± SD; $n = 3$, $^{**}P < 0.01$) in the parental cells growing in 2D adherent culture and sphere cells cultured with EGF/bFGF/B27. (*B*) MCF7 cells were incubated with EGF/bFGF/B27 with or without 5 μg/mL DHMEQ. The formed primary mammospheres were dissociated into single cells and grown as secondary mammospheres without treatment with DHMEQ. The formed mammospheres were counted, and the percentage of mammosphere-forming cells was determined (data are mean ± SD; $n = 4$, $^{**}P < 0.01$, relative to the values in the respective controls). (*C*) MCF7 cells expressing the indicated lentiviral vectors were incubated with EGF/bFGF/B27, and the formed primary mammospheres were dissociated into single cells and grown as secondary mammospheres. This process was repeated three times. The percentage of mammosphere-forming cells was determined (data are mean ± SD; $n = 4$, $^{**}P < 0.01$, relative to the values in the respective controls).

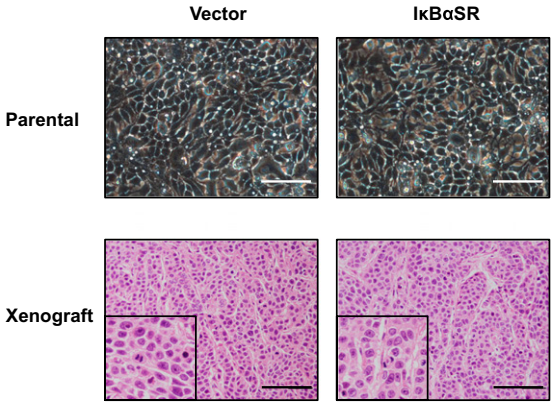

Fig. S6. Morphology of MCF7 cells expressing mutant IκBα or control vector in in vitro and histological findings of xenografted tumors. (*Upper*) Phase-contrast images of MCF7 cells expressing the control vector (*Left*) and mutant IκBα (*Right*). (*Lower*) Hematoxylin/eosin (H&E)–stained sections of tumor xenografts derived from MCF7 cells. NOD/SCID mice injected with these cells were killed after 3 wk. Scale bar = 100 μm. Both tumors showed similar histological findings. The tumors displayed a trabecular structure, and tumor cells possessed large round nuclei. In addition, both tumors had a similar mitotic index (average 4/HPF).

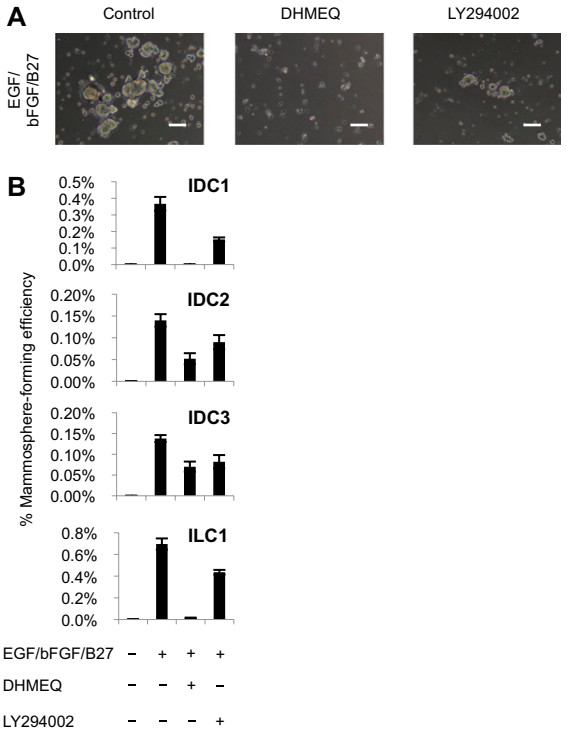

Fig. S7. NF-κB and PI3K signals control mammosphere formation of primary tumor cells derived from breast cancer patients in EGF/bFGF/B27-containing medium. (*A*) Representative images of primary cultures of mammospheres incubated with EGF/bFGF/B27, together with 5 μg/mL DHMEQ and 5 μM LY294002. Scale bar = 100 μm. (*B*) Cells from three invasive ductal carcinoma (IDC) patients (IDC1, 2, and 3) and one invasive lobular carcinoma (ILC) patient (ILC1) were treated as indicated in *A,* and the percentage of mammosphere-forming cells was determined (data are mean ± SD; *n* = 4).

Table S1. Characteristics of the patients

Patient	Age (y)	Diagnosis	Stage	Tumor size (cm)	ErbB2
IDC1	72	Invasive ductal carcinoma	IIA	2.5 × 2.0 × 2.0	1+
IDC2	87	Invasive ductal carcinoma	IIA	3.5 × 3.0 × 2.5	0–1+
IDC3	58	Invasive ductal carcinoma	IIA	2.5 × 2.0 × 1.5	1+
ILC1	72	Invasive lobular carcinoma	IA	1.6 × 1.5 × 1.5	1+

ErbB2, ErbB2 expression level (0–3+).